Journal of South American Earth Sciences 32 (2011) 567–574

Contents lists available at ScienceDirect

Journal of South American Earth Sciences

journal homepage: www.elsevier.com/locate/jsames

Age and composition of granulite xenoliths from Paso de Indios, Chubut province, Argentina

Antonio Castro [a,*], Eugenio Aragón [b], Juan Díaz-Alvarado [c], Idael Blanco [d], Antonio García-Casco [d], Katharina Vogt [e], D-Y. Liu [f]

[a] Departamento de Geología, Universidad de Huelva, Campus del Carmen, 21071 Huelva, Spain
[b] Centro de Investigaciones Geológicas (UNLP-CONICET), Facultad de Ciencias Naturales y Museo (UNLP) La Plata, Buenos Aires, Argentina
[c] Departamento de Geodinámica y Paleontología, Universidad de Huelva, Campus del Carmen, 21071 Huelva, Spain
[d] Departamento de Mineralogía Petrología, Universidad de Granada, Spain
[e] Institute of Geophysics, ETH-Zurich, Switzerland
[f] Beijing SHRIMP Center, Chinese Academy of Geological Sciences, Beijing, PR China

ARTICLE INFO

Article history:
Received 30 August 2010
Accepted 5 June 2011

Keywords:
Granulite xenoliths
Lower crust
Jurassic magmatism
South America

ABSTRACT

Granulite xenoliths enclosed in Paleogene alkali basalts from the locality of Paso de Indios in The Argentinean Patagonia, have been studied for petrology, geochemistry and U–Pb SHRIMP zircon geochronology. These are lower crust xenoliths composed of pyroxene and plagioclase dominantly. Symplectitic overgrowths with olivine and new pyroxene-plagioclase formation around the large pyroxene crystals are common. The study of phase equilibrium yields a decompression path from pressure 0.9 GPa at temperatures of about 1000 °C. The major element composition does not correspond with any known basaltic or andesitic magmas. They have $SiO_2 < 50$ wt% and MgO = 6 wt% and lower, very close in composition to the bulk lower continental crust composition. They are extremely depleted in incompatible elements with values as low as Rb = 15.3 to 4.1 ppm; Y = 6.2 to 2.5 ppm; Th = 0.92 to 0.13 ppm; U = 0.51 to 0.22 ppm; ΣREE = 53 ppm. This depletion is attributed to a residual origin of the granulites. In situ age determination with SHRIMP yields a Concordia age of 175.9 ± 4.9 Ma with MSWD = 1.4. This age represent the time of complex lithosphere evolution in relation with the formation of this residual crust.

1. Introduction

Our knowledge of the composition of the mostly unexposed lower continental crust is largely based on the analyses of granulite xenoliths dragged by basalts (Rudnick and Gao, 2003). The fast ascent of this low-viscosity, generally alkali basalts preclude decompression reactions, as well as any significant chemical interchange with the host magma. Consequently, lower crust xenoliths record unmodified fossil lower crustal conditions and compositions and their study is of great value to constrain geochemical models about the origin of the continental crust (Gao et al., 1998; Taylor and Mclennan, 1985; Weaver and Tarney, 1980) and the tectonic processes that operated in the past. However, geochronologic studies of lower crust xenoliths are scarce and, consequently, the tectonic meaning of determined paleo-pressures and paleo-temperatures, as well as compositions, remains in most cases controversial. In this paper it is presented a whole petrological and geochronologic study, based on SHRIMP U–Pb isotopic determinations, of lower crust xenoliths enclosed in Paleogene alkali basalts at Paso de Indios (Chubut province, Argentina). Our results may contribute to the better understanding of the origin and evolution of the lower crust and its implications in magmatic processes related to periods of active subduction, continental break up and potentially associated crustal reworking in this region. Apart from lower crust xenoliths, the basalts also contain upper mantle xenoliths of peridotites, dunites, and pyroxenites. These are not included in this study. However, their presence is of interest because they report that the region beneath the sampled crustal xenoliths is the mantle. So, crustal xenoliths in this locality represent, at least in part, rocks of the lowermost part of the continental crust. An important motivation for this study was to establish a correlation between processes operating in the lower crust and processes related to silicic and intermediate magma production. To address this correlation a precise age determination is required.

* Corresponding author.
E-mail address: dorado@uhu.es (A. Castro).

0895-9811/$ – see front matter © 2011 Elsevier Ltd. All rights reserved.
doi:10.1016/j.jsames.2011.06.001

2. The Paso de Indios locality. Regional setting

The Paso de Indios locality is placed at the axis of the Cañadon Asfalto rift basin of mid-upper Jurassic age (Figari and Courtade, 1993), the sedimentation of this basin is intruded and covered by mid-upper Jurassic of the Extra-Andean Volcanic rocks (Fig. 1) of Lonco Trapial, Taquetren and Alvar Formations (Nullo, 1983; Nullo and Proserpio, 1975; Rapela et al., 2005; Aragón et al., 2003), sedimentary rocks of the Upper Cretaceous Chubut group and plateau basalts of late Creataceous and Tertiarry age. The sampled unit is part of the Late Cretaceous-Paleogene alkali plateau basalts and feeding dikes at the Paso de Indios locality. Basaltic materials overlay and intrude sedimentary rocks of the Upper Cretaceous Chubut group (Alric et al., 2002). The sampled xenolith site is located at S 43° 38.570′ W 68° 593′ (Fig. 1). This locality consists of a dike of alkali basalt that corresponds to the Paleogene eruptive episode of the Vasconia Formation (Nullo, 1983). Most of these lavas carry lherzolites, harzburgites and dunites (spinel-facies) and mafic granulitic xenoliths of variable sizes but usually not greater than 5 cm, with the exception of Cerro Chenque dike in the same locality, which may contain larger granulite xenoliths up to 15 cm diameter. Fourteen $^{40}Ar/^{39}Ar$ ages of the host basalts yield ages within the range 62.50 ± 0.26 to 49.6 ± 0.77 Ma (Alric et al., 2002). Even though the Cerro Chenque outcrop was not dated, Alric et al. (2002) included this outcrop within the Eocene group (52 Ma) using geochemical criteria. These alkali basalts are related to the Paleogene synextensional bimodal volcanism of Piedra Parada volcanic complex (Aragón et al., 2005) consisting of Eocene alkali basalts and Eocene calc-alkaline rhyolite-ignimbrite plateaux at the eastern boundary of the Tertiary Ñirihuau basin (Cazau et al., 1989). Patagonia has a protracted basaltic plateau activity from upper Cretaceous to Paleogene and Neogene times. Nevertheless, xenolith-bearing (mantle and granulite) basalts are not very frequent in the region. Fig. 1 shows the most known xenolith-bearing sample localities in southernmost portion of South America. Most of them are Miocene and Neogene basalts, with the exception of the Eocene Cerro Chenque locality at Paso de Indios that is the oldest known xenolith-bearing locality. Other well known alkali basalts localities that carry ultramafic and granulite xenoliths are (Fig. 1): (1) the Pali-Aike (Selverstone and Stern, 1983) with mafic granulite xenoliths (spinel-facies) found in Pleistocene alkali basalts and suggesting a Jurassic age for the granulites, (2) the Gobernador Gregores (Rivalenti et al., 2004) with lherzolites and harzburgites hosted by Pliocene-to-recent basalts, (3) the Cerro de los Chenques (Rivalenti et al., 2007) with lherzolites, hazburgites and dunites (spinel-facies) and (4) the Prahuaniyeu (Bjerg et al., 2009) with garnet and spinel facies peridotites in Miocene basalts. A Re-Os isotopic age survey of the most important

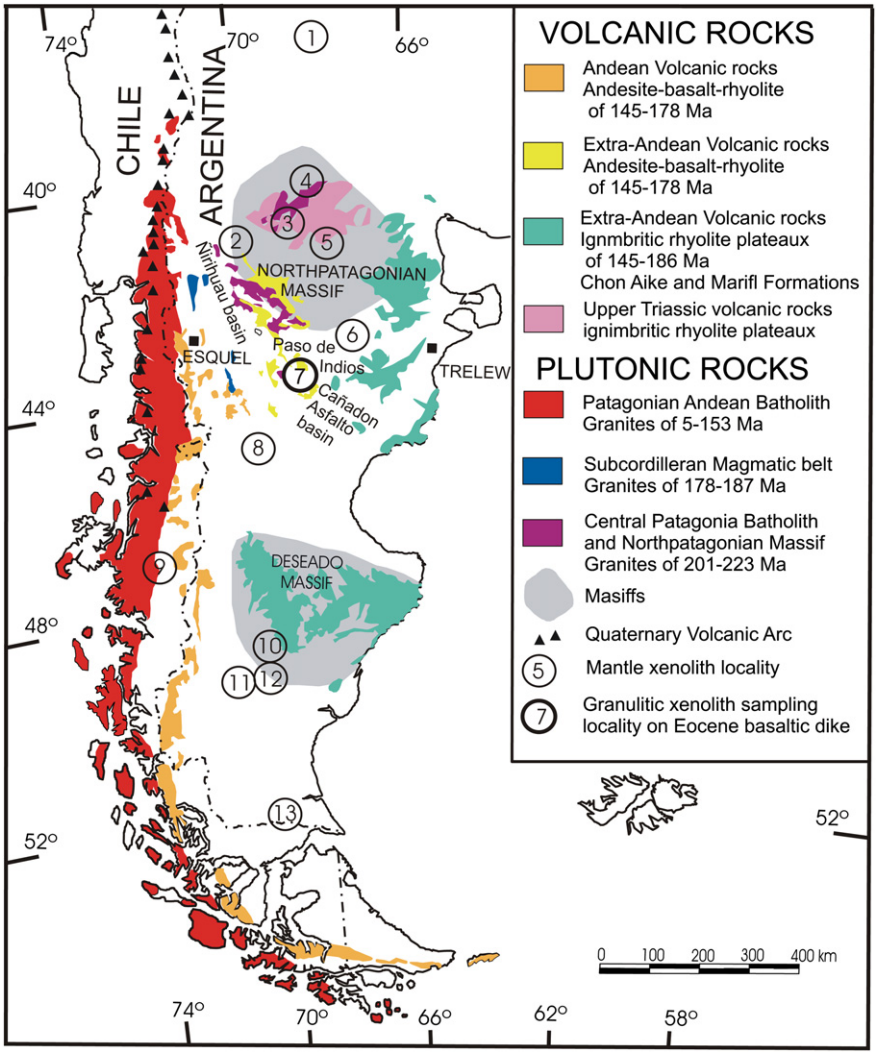

Fig. 1. Localities of lower crust and mantle xenoliths in alkali basalts in Argentina and Chile.

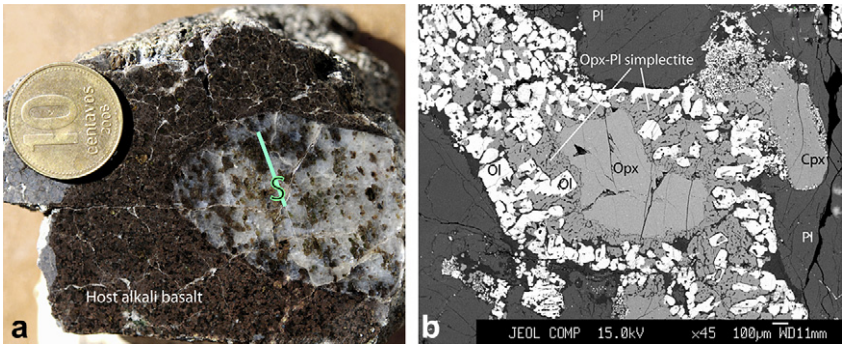

Fig. 2. (a) Polished section of a granulite xenolith at Paso de Indios showing a metamorphic foliation. (b) Back-scattered electron image (Z-contrast) showing the Ol-rich corona reaction around exsolved Opx. Symplectitic overgorowth of Pl and new Opx (darker) is associated to the same decompression corona reaction.

ultramafic xenolith localities was carried on by Schilling et al. (2008) reporting Phanerozoic depletion model ages for most of the back arc localities, with the exception of two Proterozoic depletion model ages at the North Patagonian and Deseado massifs, suggesting that the time of mantle depletion is associated with lithosphere formation.

3. Sampling and analytical techniques

Xenoliths of up to 10 cm diameter, mostly composed of pyroxene and plagioclase, were sampled at Cerro Chenque outcrop at the locality of Paso de Indios, in the Argentinean Patagonia. Note that this locality is different of the Cerro de los Chenques, which was sampled and studied by Rivalenti et al. (2007). To avoid confusion we have chosen to call the locality of this study with the local name of Paso de Indios. More than 50 individual xenoliths were collected in the same outcrop. A selected set of representative samples, according to macroscopic variations in color index and grain size, was studied for petrology, isotope geochemistry and U–Th–Pb zircon dating with Sensitive High Resolution Ion Microprobe (SHRIMP).

Major elements and Zr were analyzed by X-Ray fluorescence (XRF) at the University of Oviedo (Spain) using glass beads. Precision of the XRF technique was better than ±1.5% relative. Trace element and rare earth elements (REE) were analyzed by inductively coupled plasma mass spectrometry (ICP-MS) with an HP-4500 system at the University of Huelva, following digestion in an HF + HNO_3 (8:3) solution, drying and second dissolution in 3 ml HNO_3. The average precision and accuracy for most of the elements were controlled by repeated analyses of SARM-1 (granite) and SARM-4 (norite) international rock standards. They fall in the range of 5–10% relative. Probe analyses were obtained with a JEOL JXA-8200 SuperProbe at the University of Huelva. A combination of silicates and oxides were used for calibration.

Zircon separation was accomplished by traditional techniques using dense liquids and magnetic (Franz) separation. Selected crystals free of impurities and fractures were selected by hand-picking with a binocular lens. These were mounted in epoxy, together with reference standards, and polished. Sectioned zircons were studied by CL imaging for selection of point analyses. Core and rims were analyzed in several grains of each individual sample with the aim of identifying inherited cores. These selected points were target over the CL images and analyzed for U–Th–Pb isotopes with SHRIMP at the Beijing-SHRIMP Center (Chinese Academy of Geological Sciences, Beijing), following methods given in Williams (1998) and references therein. The data were processed with ISOPLOT software (Ludwig, 2003) for Concordia plots, probability density plots, stacked histograms and weighted means and Concordia age calculations.

Table 1
Whole-rock analyses of major and trace elements of granulite xenoliths of Paso de Indios (Patagonia).

Muestra	E909-6.3A	E909-6.3B	BLC[a]
(wt.%)			
SiO_2	48.33	48.57	53.40
TiO_2	0.84	–	0.82
Al_2O_3	18.57	24.2	16.90
FeOt	8.48	5.05	8.57
MgO	6.37	5.76	7.24
MnO	0.12	0.07	0.11
CaO	10.67	12.93	9.59
Na_2O	2.70	1.84	2.65
K_2O	1.31	0.43	0.61
P_2O_5	0.31	0.16	0.10
Loi	1.01	–	0.24
TOTAL	98.71	99.26	99.99
Mg#[b]	0.57	0.67	0.60
(ppm)			
Li	5.69	15.9	13
Be	0.89	0.11	1.4
Sc	23.1	19.1	31
V	217	113	196
Cr	72.7	364	215
Co	30.7	24.2	38
Ni	46.1	57.1	88
Cu	123	15.8	26
Zn	44.5	26.1	78
Ga	18.9	16.6	13
Rb	15.3	4.06	11
Sr	606	1301	348
Y	6.21	2.47	16
Zr	41.5	11.5	68
Nb	7.73	0.74	5
Cs	0.24	0.06	0.3
Ba	243	82.5	259
La	9.49	1.84	8
Ce	24.9	3.70	20
Pr	2.40	0.46	2.4
Nd	8.42	2.11	11
Sm	1.83	0.52	2.8
Eu	0.89	0.30	1.1
Gd	1.80	0.50	3.1
Tb	0.27	0.08	0.5
Dy	1.42	0.45	3.1
Ho	0.31	0.09	0.7
Er	0.70	0.24	1.9
Tm	0.12	0.04	0.2
Yb	0.62	0.23	1.5
Lu	0.10	0.04	0.3
Hf	1.29	0.34	1.9
Ta	1.00	0.09	0.6
W	39.3	–	0.6
Pb	4.72	1.26	4
Th	0.92	0.13	1.2
U	0.51	0.22	0.2

[a] Bulk composition of the lower continental crust (Rudnick and Gao, 2003).
[b] Mg# = Mol MgO/(MgO + FeO).

4. Granulite xenoliths. Petrography and PT evolution

Xenolits have irregular and rounded shape, ranging in size from 3 cm to 10 cm. They do not show appreciable reaction with host basalt and no zoning or reaction aureoles with the host basalt (Fig. 2a), few have microscopic veins of basalt. They are medium-grained granular rocks essentially composed of plagioclase (Pl), orthopyroxene (Opx) and clinopyroxene (Cpx) with subordinate olivine (Ol), zircon (Zrn) and apatite (Ap) (mineral abbreviations according to Kretz, 1983). Some samples contain green and brown spinel (Spl). They are often equigranular and isotropic rocks, but some samples show a parallel banding of mafic minerals resembling a metamorphic foliation (Fig. 2a). All of then have granoblastic texture with frequent corona textures defined by reaction aureoles with olivine + plagioclase + pyroxene symplectites surrounding pyroxene crystals. Results of the whole rock compositions are given in Table 1. Representative mineral compositions are given in Table 2. The study of the reaction coronas is addressed here in order to determine the pressure-temperature evolution. The interest of these determinations is that they can be ascribed to a particular period of crustal evolution at the age reported by precise zircon geochronology.

4.1. Mineral compositions and PT evolution

The peak mineral assemblage is formed by clinopyroxene, orthopyroxene, plagioclase, ilmenite and spinel, overprinted by late retrograde olivine + plagioclase coronas (Fig. 2b) developed around the pyroxenes, and retrograde K-feldspar localized, mostly, in fractures and patches adjacent to plagioclase. Pyroxenes appear reequilibrated and exsolved. Clinopyroxene have Al- and Na-poorer rims and patchy core regions adjacent to exsolved orthopyroxene/ilmenite, while patchy relictic compositions distributed in the cores have up to 0.31 Al and 0.06 Na per 6 oxygens (Fe = Fe^{2+}_{total}). Similarly, orthopyroxene bear Al-poorer and Ca-richer rims and patchy core regions adjacent to clinopyroxene exsolutions, having up to 0.20 Al per 6 oxygens in relictic patchy core regions. The anorthite content of plagioclase ranges 0.66–0.86, with higher values in plagioclase associated to olivine in coronas. The forsterite content of olivine ranges 0.61–0.66.

P-T conditions were estimated using an isochemical P-T projection (pseudosection) computed with software PerpleX (Connolly, 2005) in the system TiNCFMAS. The bulk rock composition of the sample (Table 1) was slightly transformed in order to account the Si and Al contents present in retrograde K-feldspar (not considered in the calculations): SiO_2 = 52.68, TiO_2 = 0.72, Al_2O_3 = 11.52, FeO_{tot} = 8.12, MgO = 10.87, CaO = 13.09, Na_2O = 2.99 (molar proportions). Thermodynamic data were taken from the internally consistent database of Holland and Powell (1998). Solid solutions considered are from Holland and Powell (1998) for olivine, Holland and Powell (1996) for orthopyroxene and clinopyroxene, and Newton et al. (1980) for high structural state plagioclase. Spinel and ilmenite were treated as ideal Fe–Mg solid solutions.

The thermodynamic predictions indicate that clinopyroxene, ortopyroxene, plagioclase and ilmenite are stable at higher pressure while olivine joins the assemblage at pressure below 0.9 GPa (Fig. 3). The distribution of phase assemblages and mineral

Table 2
Representative compositions of minerals.

Phase	Cpx	Cpx	Opx	Opx	Ol	Ol	Pl	Pl
Type	Core (highest Al and Na)	rim (lowest Al and Na)	Core (highest Al)	Corona	Corona	Corona	Matrix	Corona
SiO_2	48.05	49.44	50.95	54.17	36.31	36.32	50.80	46.15
TiO_2	1.02	1.17	0.15	0.18	0.02	0.00		
Al_2O_3	7.09	4.43	4.48	0.22	0.06	0.01	31.50	35.06
Cr_2O_3	0.03	0.00	0.01	0.00	0.05	0.04		
FeO_{tot}	7.91	9.11	20.22	19.38	30.26	33.44	0.33	0.26
MnO	0.14	0.11	0.34	0.33	0.39	0.60		
MgO	12.40	12.39	24.09	24.57	33.47	30.20		
NiO	0.01	0.00	0.02	0.00	0.02	0.02		
CaO	22.04	22.69	0.43	1.86	0.15	0.14	13.50	17.32
Na_2O	0.88	0.38	0.01	0.04	0.01	0.01	3.75	1.58
K_2O	0.00	0.00	0.00	0.00	0.01	0.02	0.10	0.03
Total	99.57	99.73	100.69	100.75	100.76	100.79	99.97	100.39
Si	1.78	1.85	1.85	1.97	0.97	0.99	2.31	2.11
Ti	0.03	0.03	0.00	0.00	0.00	0.00		
Al	0.31	0.20	0.19	0.01	0.00	0.00	1.69	1.89
Cr	0.00	0.00	0.00	0.00	0.00	0.00		
Fe^{3+}[a]	0.13	0.06	0.09	0.03	0.05	0.02	0.01	0.01
Fe^{2+}[a]	0.12	0.22	0.52	0.56	0.63	0.74	0.00	0.00
Mn	0.00	0.00	0.01	0.01	0.01	0.01		
Mg	0.69	0.69	1.31	1.33	1.33	1.23		
Ni	0.00	0.00	0.00	0.00	0.00	0.00		
Ca	0.88	0.91	0.02	0.07	0.00	0.00	0.66	0.85
Na	0.06	0.03	0.00	0.00	0.00	0.00	0.33	0.14
K	0.00	0.00	0.00	0.00	0.00	0.00	0.01	0.00
O	6.00	6.00	6.00	6.00	4.00	4.00	8.00	8.00
$Mg/(Mg + Fe^{2+})$	0.85	0.76	0.71	0.71	0.68	0.62		
Fe_{tot}	0.25	0.29	0.62	0.59	0.68	0.76	0.01	0.01
Wo	48.36	48.14	0.86	3.62				
En	37.85	36.58	67.03	66.46				
Fs	13.79	15.28	32.11	29.92				
An							0.66	0.86
Ab							0.33	0.14
Or							0.01	0.00

[a] Calculated by stoichiometry. Pyroxene end-members calculated following Morimoto et al (1988).

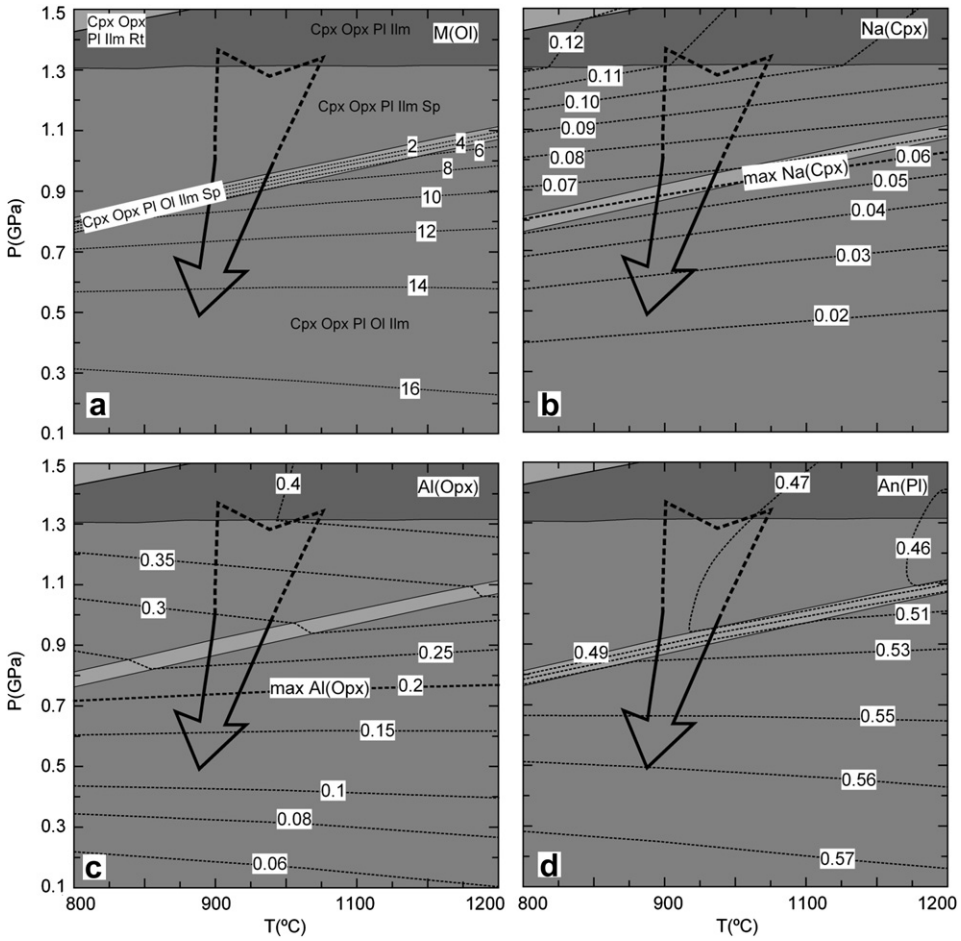

Fig. 3. Isochemical P-T equilibrium phase diagram for studied sample calculated with Perplex with indication of (a) isopleths of mole proportion of olivine, (b) Na-in-clinopyroxene, (c) Al-in-orthopyroxene and (d) XAn in plagioclase. Mineral code: Ol (olivine), Cpx (clinopyroxene), Opx (orthopyroxene), Pl (plagioclase), Ilm (ilmenite), Sp (spinel). Color code: thermodynamic variance (light gray: 3-variant; dark gray: 5-variant). The P-T path is indicated by (thick arrow). (For interpretation of the references to colour in this figure legend, the reader is referred to the web version of this article.)

abundance isopleths indicate that the process of formation of olivine coronas involved strong decompression rather than cooling. A near-isothermal decompression P-T path would form plagioclase during olivine growth, as observed. Clinopyroxene-orthopyroxe geothermometry (Putirka, 2008), gives results in ca. 920–940 °C using different mineral–core pairs. Although these results are consistent, the absolute temperature of decompression path is uncertain given that the pyroxenes underwent reequilibration during decompression and equilibrium is not warranted. The abundance of Na in relict clinopyroxene indicate ca. 0.9 GPa at 900–1000 °C. Maximum Al in orthopyroxene indicates 0.7 GPa at similar temperature. Maximum Al in clinopyroxene indicates much lower pressure conditions (<0.3 GPa), suggesting equilibrium problems and/or problems with the thermodynamic data and/or solid solution models. However, the small dP/dT slopes of phase assemblage boundaries and mineral abundance and composition isopleths support a general near-isothermal decompression path starting at $P > 0.9$ GPa (>30 km).

5. Geochemistry and U–Pb zircon geochronology

Analytical results from two representative granulite xenoliths are shown in Table 1. Selected geochemical plots for trace elements are shown in Fig. 4 in order to make a general comparison with the composition of the lower continental crust (Rudnick and Gao, 2003; Taylor and Mclennan, 1985). According to these bulk compositional data, the most outstanding features of the Paso de Indios lower crust xenoliths areas follows:

(1) They have low silica contents (SiO_2 <50 wt%) for MgO contents about 6 wt%.
(2) The content in CaO is higher (>10 wt%) than normal in basalts but comparable to the values of the bulk lower crust composition (BLC, Table 1).
(3) They have Mg# (Mg# = mol MgO/MgO + FeO) of about 0.6 and Ni contents about 50 ppm.
(4) They are strongly depleted in incompatible elements as it is shown in the MORB-normalized plot (Fig. 4a). This depletion is more pronounced for HFSE (from Sm to Yb), with values below the bulk lower continental crust (Rudnick and Gao, 2003). The peak in Sr is related to the large abundance of plagioclase in the Paso de Indios xenoliths. Beside of being normal compared to lower crust composition, the K content of some xenoliths is relatively higher with respect to the neighboring elements in the diagram (Th and Nb). The peak in K is attributed to contamination with the K-rich (shoshonitic) host basalt. Some K-rich veins are often identified in thin sections. These are also rich in apatite, accounting for the enrichment in P (relative to Nd and Sm) displayed in the spider diagram (Fig. 4).

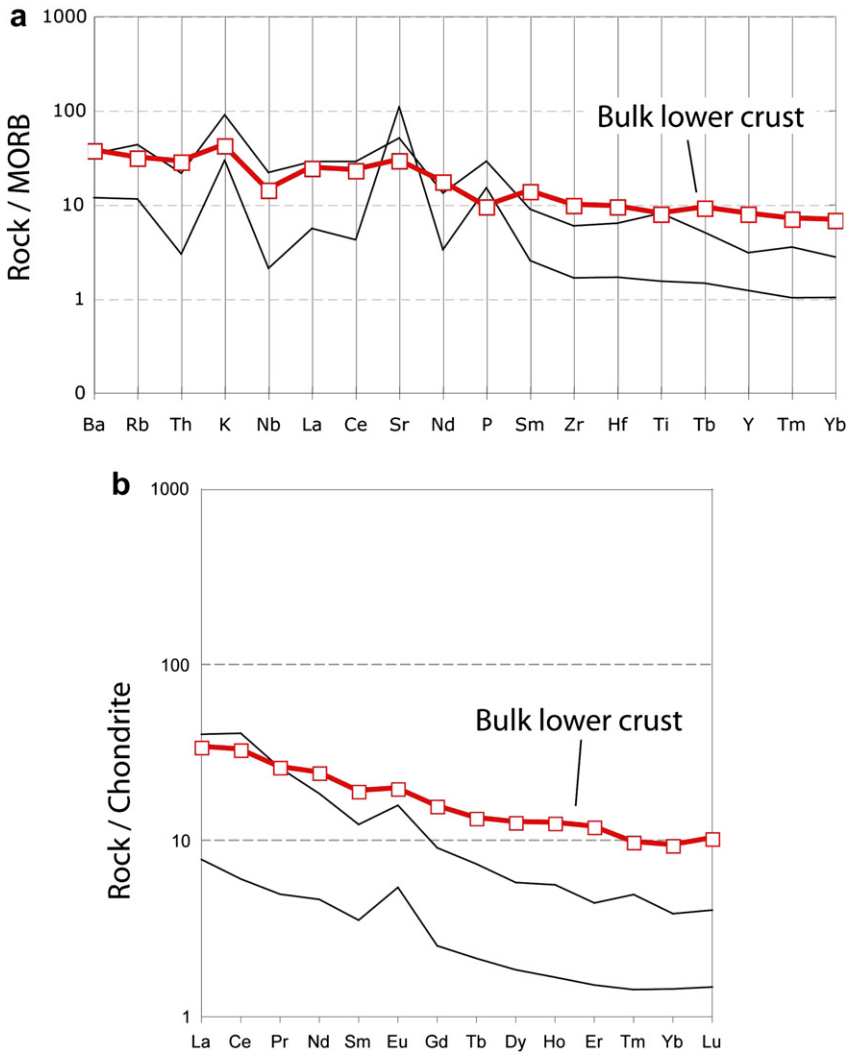

Fig. 4. Comparison of trace element compositions of the Paso de Indios xenoliths with the bulk lower continental crust (Rudnick and Gao, 2003) in (a) the MORB-normalized diagram (Thompson et al., 1984) and (b) the Chondrite-normalized (Nakamura, 1974) REE diagram.

(5) Chondrite-normalized REE patterns are characterized by a strongly depletion in HREE and a pronounced positive Eu anomaly with values of Eu/Eu* of 1.5 and 1.8 for the two analyzed xenoliths (Fig. 4b). Most REE contents are lower than the bulk lower crust composition (Rudnick and Gao, 2003).

In summary, the bulk composition of these mafic granulites (Table 1, Fig. 4) is almost coincident with the averaged composition of the lower continental crust (Rudnick and Gao, 2003; Taylor and Mclennan, 1985). This is a broadly intermediate in composition, more silicic than basalts but more mafic than granites. The studied xenoliths are also very close in composition to other granulite xenolith localities as that of Pali-Aike in Tierra del Fuego, Chile; (Selverstone and Stern, 1983) and also close to the Low-Mg mafic granulite xenoliths from California (Lee et al., 2006, 2007).

Zircon crystals are very scarce in these granulite xenoliths due to the strong depletion in Zr (<42 ppm) and the rest of HFSE incompatible elements. This limitation, together with the small size of xenoliths, make hard to get only few crystals to study for zoning and geochoronology. Selected grains for U–Pb SHRIMP analyses are mostly euhedral to subhedral prismatic crystals. Acicular and elongated crystals are less common. They lack inherited cores and the observed overgrowths are continuous, only disrupted by the abundant inclusions. Seven point analyses were made (Table 3) providing a Concordia age of 175.9 ± 4.9 Ma with MSWD = 1.4 (Fig. 5).

6. Discussion and concluding remarks

All these xenoliths have in common an abnormal composition compared to common magmas. In spite they have silica contents close to basaltic compositions (ca. 50 wt%), they have values of MgO (<6.0%) that are too low for basaltic magmas. Andesites with these low MgO contents are richer in silica (SiO_2> 55 wt%) than lower crust granulites. After rejection of possible genetic mechanisms as reaction products and primitive melts, they more likely represent solid residues left after segregation of a silicic melt by either partial melting of a solid source or incomplete crystallization of a parental intermediate magma. The strong depletion in incompatible elements (Rb = 15.3 to 4.1 ppm; Y = 6.2 to 2.5 ppm; Th = 0.92 to 0.13 ppm; U = 0.51 to 0.22 ppm; ΣREE = 53 ppm; Table 1) is similar to other lower crust mafic granulites. The composition of this extracted melt cannot be determined by direct methods. However, the comparison between the composition of these residual xenoliths with the average compositions of restites in melting experiments with composite sources of mixed layers (Bt-rich + amphibolite)

Table 3
Summary of SHRIMP U–Pb zircon data for sample E909-6.3.

Grain and spot	^{206}Pb (ppm)	^{206}Pb$_c$ %	^{238}U (ppm)	^{232}Th (ppm)	Th/U	^{206}Pb/^{238}U	± %	^{207}Pb/^{235}U	± %	^{207}Pb/^{206}Pb	± %	^{206s}Pb/^{238}U age (Ma)	±
1,1	6.10	0.78	250	120	0.49	0.02816	2.5	0.199	5.0	0.0512	4.3	179.0	4.5
2,1	4.86	0.14	202	78	0.40	0.02795	2.6	0.219	3.9	0.0567	3.0	177.7	4.5
3,1	7.72	0.13	307	93	0.31	0.02925	2.5	0.221	3.5	0.0548	2.4	185.9	4.6
4,1	7.37	0.18	314	163	0.54	0.02727	2.5	0.198	3.8	0.0526	2.8	173.4	4.3
5,1	5.57	1.51	232	82	0.36	0.02749	2.6	0.186	9.6	0.0491	9.3	174.8	4.5
5,2	4.43	1.80	187	74	0.41	0.02710	2.6	0.193	9.4	0.0518	9.0	172.4	4.5
6,1	5.84	1.00	252	104	0.43	0.02667	2.6	0.186	7.7	0.0506	7.3	169.7	4.3

Errors are 1-sigma.
Pbc = common Pb.
Error in Standard calibration was 0.71% (not included in above errors but required when comparing data from different mounts).
Common Pb corrected using measured ^{204}Pb in all isotopic ratios and ages.

from the subduction channel (Castro et al., 2010) indicates that the segregated melts can be of granitic to granodioritic composition.

The metamorphic evolution of these residual rocks indicates a dominant decompression pattern starting at $P > 0.9$ GPa. The most intriguing point of this decompression path is the high temperature (T = 900–1000 °C), higher than temperatures recorded in mafic granulite terrains (Harley, 1989), or predicted by normal geothermal gradients at the lower continental crust, but consistent with mobile belts temperatures at the backarc Moho of 800–900 °C (Hyndman et al., 2005). It is possible that xenoliths record peak temperatures because they are frozen by rapid exhumation by fast basalt ascent of about 6 h from the lower crust to the surface (Selverstone and Stern, 1983), compared with the several orders of magnitude slower tectonic ascent of granulite terranes. Decompression from 0.9 GPa at so high temperatures of about 1000 °C cannot be related to a purely crustal process. The implication is that a hot system represented in part by the granulite residues (xenoliths) and containing a high T melt, underwent a previous lithosphere evolution of fractionation or partial melting of an intermediate composition (andesitic) magma or rock present at the lower continental crust. The granulite xenoliths are emplaced at and are coeval to the development of the Cañadon Asfalto rift basin. The geodynamic environment of southern South America 155 Ma ago showed to the east of Paso de Indios the initial stages of break up of Gondwana (the first phases of seafloor spreading between Antartica and Africa happened about 155 Ma ago, Martin and Hartnady, 1986). Instead, to the west of Paso de Indios, subduction and a magmatic arc was developed at this latitude, documented by the volcanic rocks from the Lago de La Plata group of Taoarcian to Tithonian age (Haller and Lapido, 1980), and the emplacement of the Patagonian Andean Batholith (Pankhurst et al., 1999; Castro et al., 2011). Therefore, the Paso de Indios area represents a transition zone between continental rifting and subduction. Time space distribution of the Jurassic synextensional extra-andean volcanism shows an SW age decrease for the beginning of volcanic activity (representing one of the largest silicic provinces in the world, Féraud et al., 1999; Pankhurst et al., 2000) from NE Patagonia (186 Ma) to SW Patagonia (146 Ma). The protracted extensional regime for this region may account for some of the isothermal decompression shown by the granulite xenoliths, as a consequence of crustal thinning.

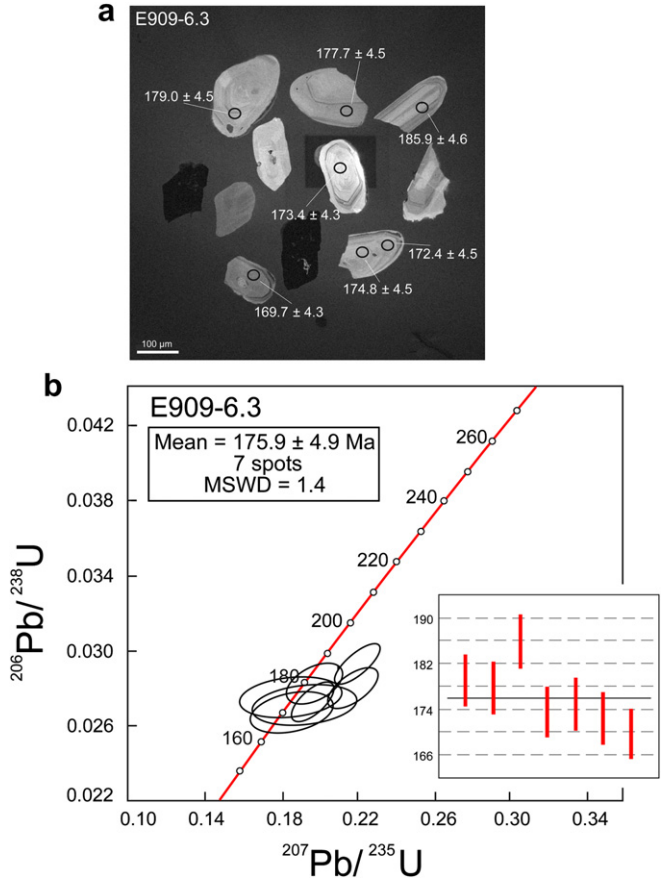

Fig. 5. (a) Cathodoluminescence (CL) images of the analyzed zircons from the granulite xenoliths of Paso de Indios. Location of the SHRIMP spots and their resulting ^{206}Pb/^{238}U ages (Ma) are indicated. (b) U–Pb Concordia diagram, including 1σ error bars plot. Data-point error ellipses are 95% confidence.

It is clear that the petrological study of these lower crust xenoliths may have large implications on geodynamic models and crustal growth processes. Interestingly, these processes are dated with relative accuracy to a period of time during Jurassic at about 176 Ma (175.9 ± 4.9 Ma) according to the zircon ages reported in this paper. This is the data to take into account to decipher the complex petrologic processes of granulite generation. This geochronologic datum can be used to correlate other tectonic and silicic magmatic processes in the region that complement general genetic models and tectonic processes. The reported age is almost coincident with the age of several Cordilleran-type granodiorite-diorite intrusions (Castro et al., 2010, 2011) and andesitic volcanic rocks in the Paso the Indios region (Aragón et al., 2003).

Acknowledgments

Sampling, petrology and SHRIMP studies were funded with research grants form the Spanish Ministry of Science and Innovation (Projects CGL2007-63237/BTE). Field-work was supported to E. Aragón with grants from projects of UNLP 11N/534, CONICET PID 00916 and PRIN-COFIN 2007.

References

Alric, V.I., Haller, M.I., Féraud, G., Betrand, H., 2002. Volcanismo Alcalino Paleógeno en los alrededores de Paso de Indios, Provincia del Chubut. Actas del XV Congreso Geológico Argentino. El Calafate. Actas 2, 101–106.

Aragón, E., Gonzalez, P., Aguilera, Y., Cavarozzi, C., Llambías, E., Rivalenti, G., 2003. Thermal Divide Andesites-trachytes, petrologic evidences and implications from North Patagonian Massif alkaline Jurassic volcanism. Journal of South American Earth Sciences 16, 91–103.

Aragón, E., Aguilera, Y., Cavarozzi, C., Ribot, A., 2005. Basaltos Alcalinos en el Complejo Volcánico-Piroclastico del Río Chubut medio. Actas XVI Congreso Geologico Argentino. Actas 1, 485–486.

Bjerg, E.A., Ntaflos, T., Thöni, M., Alían, P., Labudia, C.H., 2009. Heterogeneous lithospheric mantle beneath Northern Patagonia: evidence from Prahuaniyeu garnet-and spinel-Peridotites. Journal of Petrology 50 (7), 1267–1298.

Castro, A., Gerya, T., García-Casco, A., Fernández, C., Díaz Alvarado, J., Moreno-Ventas, I., Loew, I., 2010. Melting relations of MORB-sediment mélanges in underplated mantle wedge plumes. implications for the origin of cordilleran-type batholiths. Journal of Petrology 51, 1267–1295.

Castro, A., Moreno-Ventas, I., Fernández, C., Vujovich, G., Gallastegui, G., Heredia, N., Martino, R.D., Becchio, R., Corretgé, L.G., Díaz-Alvarado, J., García-Arias, M., Liu, D-Y, 2011. Petrology and SHRIMP U-Pb zircon geochronology of Cordilleran granitoids of the Bariloche area, Argentina. Journal of South American Earth Science 32 (4), 508–530.

Cazau, L., Mancini, D., Cangini, J., Spallettil, L., 1989. Cuenca Ñirihuau. In: Chebli, G., Spalletti, L. (Eds.), Cuencas Sedimentarias de Argentina, Correlación Geológica, 6, pp. 299–318.

Connolly, J.A.D., 2005. Computation of phase equilibria by linear programming: a tool for geodynamic modeling and its application to subduction zone decarbonation. Earth and Planetary Science Letters 236, 524–541.

Féraud, G., Alric, V., Fornari, M., Bertrand, H., Haller, M., 1999. $^{49}Ar/^{39}Ar$ dating of the Jurassic volcanic province of Patagonia: migrating magmatism related to Gondwzna break.up and subduction. Earth and Planetary Science Letters 172, 83–96.

Figari, E.G., Courtade, S.P., 1993. Evolución tectosedimentaria de la cuenca de Cañadon Asfalto, Chubut, Argentina. 12o Congreso Geológico Argentino y 2° Congreso de Exploración de Hidrocarburos. Actas1: 66-77.

Gao, S., Zhang, B.-R., Jin, Z.-M., Kern, H., Ting-Chuan, L., Zhao, Z.-D., 1998. How mafic is the lower continental crust? Earth and Planetary Science Letters 161, 101–117.

Haller, M.J., Lapido, O.R., 1980. El Mesozoico de la Cordillera Patagonica Central. Revista de la Asociación Geológica Argentina 35, 230–247.

Harley, S.L., 1989. The origins of granulites: a metamorphic perspective. Geological Magazine 126, 215–247.

Holland, T.J.B., Powell, R., 1996. Thermodynamics of order-disorder in minerals. 2. Symmetric formalism applied to solid solutions. American Mineralogist 81, 1425–1437.

Holland, T.J.B., Powell, R., 1998. An internally consistent thermodynamic data set for phases of petrological interest. Journal of Metamorphic Geology 16, 309–343.

Hyndman, R.D., Currie, C.A., Mazzotti, S.P., 2005. Subduction zone back arcs, mobile belts, and orogenic heat. GSA Today 15, 4–10.

Kretz, 1983. Symbols for rock-forming minerals. American Mineralogist 68, 277–279.

Lee, C.T.A., Cheng, X., Horodyskyj, U., 2006. The development and refinement of continental arcs by primary basaltic magmatism, garnet pyroxenite accumulation, basaltic recharge and delamination: insights from the Sierra Nevada, California. Contributions to Mineralogy and Petrology 151, 222–242.

Lee, C.T.A., Morton, D.M., Kistler, R.W., Baird, A.K., 2007. Petrology and tectonics of Phanerozoic continent formation: from island arcs to accretion and continental arc magmatism. Earth and Planetary Science Letters 263, 370–387.

Ludwig, K.R., 2003. Mathematical-statistical treatment of data nd errors for Th-230/U geochronology. Uranium-Series Geochemistry. Rewiews in Mineralogy and Geochemistry 52, 631–656.

Martin, A.K., Hartnady, C.J.H., 1986. Plate tectonic development of the South Indian Ocean: a revised reconstruction of east Antartica and Africa. Journal of Geophysical Research 91, 4767–4786.

Morimoto, N., Fabries, J., Ferguson, A.K., Ginzburg, I.V., Ross, M., Seifert, F.A., Zussman, J., Aoki, K., Gottardi, G., 1988. Nomenclature of pyroxenes: Report of the Subcommittee on Pyroxenes of the International Mineralogical Association, Commission on New Minerals and Mineral Names. American Mineralogist 73, 1123–1133.

Nakamura, N., 1974. Determination of REE, Ba, Fe, Mg, Na and K in carbonaceous and ordinary cohondrites. Geochimica et Cosmochimica Acta 38, 757–775.

Newton, R.C., Charlu, T.V., Kleppa, O.J., 1980. Thermochemistry of the high structural state plagioclases. Geochemica et Cosmochimica Acta 44, 933–941.

Nullo, F.E., 1983. Descripción Geológica de la Hoja 45c, Pampa de Agnia, Provincia de Chubut. Servicio Geológico Nacional. Boletín N° 199, 1–99.

Nullo, F.E., Proserpio, C., 1975. La Formación Taquetren en Cañadón del Zaino (Chubut) y sus relaciones estratigráficas en el ámbito de la Patagonia de acuerdo a la flora. Revista de la Asociación Geológica Argentina 30 (2), 133–150.

Pankhurst, R.J., Weaver, S.D., Hervé, F., Larrondo, P., 1999. Mesozoic-Cenozoic evolution of the North Patagonian Batholith in Aysén, southern Chile. Journal of the Geological Society 156, 673–694. London.

Pankhurst, R.J., Riley, T.R., Fanning, C.M., Kelley, S.P., 2000. Episodic silicic volcanism in Patagonia and the Antartic Peninsula: chronology of magmatism associated with the break-up of Gondwana. Journal of Petrology 41, 605–625.

Putirka, K.D., 2008. Thermometers and Barometers for volcanic Systems. Reviews in Mineralogy and Geochemistry 69, 61–120.

Rapela, C.W., Pankhurst, R.J., Fanning, C.M., Hervé, F., 2005. Pacific subduction coeval with the Karoo mantle plume: the Early Jurassic Subcordilleran belt of northwestern Patagonia. In: Vaughan, A.P.M., Leat, P.T., Pankhurst, R.J. (Eds.), Terrane Processes at the Margins of Gondwana. Geological Society, London, Special Publications, vol. 246 217–239.

Rivalenti, G., Mazzucchelli, M., Laurora, A., Ciuffi, S.L.A., Zanetti, A., Vannucci, R., Cingolani, C., 2004. The backarc mantle lithosphere in Patagonia, South America. Journal of South American Earth Sciences 17, 121–152.

Rivalenti, G., Mazzucchelli, M., Zanetti, A., Vannucci, R., Bollinger, C., Hémond, Ch., Bertotto, G.W., 2007. Xenoloths from Cerro de los Chenques (Patagonia): an example of slab-related metasomatim in the backarc lithospheric mantle. Lithos 99, 45–67.

Rudnick, R.L., Gao, S., 2003. Composition of the continental crust. In: Rudnick, R.L. (Ed.), The Crust. Elsevier-Pergamon: Oxford, pp. 1–64.

Schilling, M.E., Carlson, R.W., Conceiçâo, R.V., Dantas, C., Bertotto, G.W., Koester, E., 2008. Re-Os isotope constraints on subcontinental lithospheric mantle evolution of southern South America. Earth and Planetary Science Letters 268, 89–101.

Selverstone, J., Stern, C.R., 1983. Petrochemistry and recrystallization history of granulite xenoliths from the Pali-Aike volcanic field, Chile. American Mineralogist 68, 1102–1112.

Taylor, S.R., Mclennan, S.M., 1985. The continental crust: its composition and evolution. Blackwell, Melbourne.

Thompson, R.N., Morrison, M.A., Hendry, G.L., Parry, S.J.P., 1984. An assessment of the relative roles of a crust and mantle in magma genesis: an elemental aproach. Philosophical Transaction of the Royal Society of London 590, 549–590. A310. P549.

Weaver, B.L., Tarney, J., 1980. Continental crust composition and nature of the lower crust: constraints from mantle Nd-Sr isotope correlation. Nature 286, 342–346.

Williams, L.S., 1998. U-Th-Pb geochronology by ion microprobe. In: McKibben, M.A., Shanks, W.C., Ridley, W.L. (Eds.), Applications of Microanalytical Techniques to Understanding Mineralizing Processes. Reviews in Economic Geology, 7, pp. 1–35.